Full Length Research Article
Advancements in Life Sciences – International Quarterly Journal of Biological Sciences

ARTICLE INFO

Date Received: 18/02/2025;
Date Revised: 04/11/2025;
Available Online: 28/12/2025;

Author's Affiliation:
Department of Clinical Laboratory Sciences, College of Applied Medical Sciences, King Saud University, Riyadh 11362 – Saudi Arabia

***Corresponding Author:**
Abdulhadi M Abdulwahed
Email: Aabdulwahed@ksu.edu.sa

How to Cite:
Abdulwahed AM (2025). Directing Cancer-Related Angiogenesis: Progressive E-Pharmacophore Modelling of Novel Selective VEGFR-1 Inhibitors. Adv. Life Sci. 12(4): 780-790.

Keywords:
VEGFR-1; Angiogenesis; Benzamide; Pharmacophore modelling; Molecular docking; Virtual screening

Open Access

Directing Cancer-Related Angiogenesis: Progressive E-Pharmacophore Modelling of Novel Selective VEGFR-1 Inhibitors

Abdulhadi M Abdulwahed

Abstract

Background: Vascular endothelial growth factor receptor-1 (VEGFR-1) is a tyrosine kinase receptor that plays a key role in angiogenesis signalling. Development of selective VEGFR-1 inhibitors represents a promising anti-angiogenic therapeutic strategy for cancer treatment. However, design of selective VEGFR-1 inhibitors remains challenging.

Methodology: The crystal structure of VEGFR-1 kinase domain bound to an inhibitor (PDB: 3HNG) was pre-processed using Protein Preparation Wizard tools in Schrodinger. Missing loops were modelled and hydrogen atoms added at pH 7.0. Minimization gently refined the structure. A receptor-based pharmacophore model was developed using Phase to elucidate geometry and physicochemical requirements for inhibition based on the complex structure.

Results: Database screening was conducted by flexibly fitting 896 lead-like compounds from PubChem onto the pharmacophore and scoring for optimal alignment. Top-scoring hits were docked into the VEGFR-1 binding site using Glide SP precision protocol, allowing ligand flexibility. Affinity was predicted via physics-based scoring functions. Pharmacophore screening retrieved hits that complemented critical hydrophobic and hydrogen bonding elements for VEGFR-1 inhibition. Docking yielded strong predicted binding energies on par with or better than the cocrystal inhibitor with screened compound CID: 9820557 taking the lead. Specific ligand-protein interactions provided a rationale for predicted potency.

Conclusion: An integrated computational approach combining pharmacophore modelling, virtual screening, and molecular docking enabled identification of promising VEGFR-1 targeted inhibitors. Further clinical research can propose these leads to develop as more selective agents against this important anti-angiogenic target.

Introduction

Angiogenesis, the formation of new blood vessels from pre-existing vasculature, is a crucial process that tumors exploit to fuel growth and enable metastasis [1]. Vascular endothelial growth factor (VEGF) signalling, through its transmembrane tyrosine kinase receptors VEGFR-1, VEGFR-2, and VEGFR-3, regulates endothelial cell proliferation, migration, and blood vessel formation, making it a master regulator of angiogenesis [2]. The essential role of VEGFR activation in promoting tumour angiogenesis has spurred development of therapeutic inhibitors targeting these pathways [3]. In particular, VEGFR-1 has garnered attention based on multi-functional contributions to angiogenesis beyond VEGFR-2 mediated endothelial proliferation. Selective VEGFR-1 inhibition suppresses migration of tip cells guiding new vessel sprouts, disrupting the vascular architecture sustaining tumor growth [4]. However, translation of VEGFR-1 inhibitors from bench to bedside has lagged behind VEGFR-2 counterparts. This study aims to improve VEGFR-1-targeted anti-angiogenic agents through structure-guided pharmacophore design to generate more effective lead candidates, thereby enhancing treatment effectiveness and expanding options.

Tyrosine kinase inhibitors (TKIs) like sunitinib, sorafenib and pazopanib displaying pan-VEGFR activity are approved for treating various malignancies [5,6]. However, their lack of selectivity leads to dose-limiting toxicities and acquires resistance over prolonged use. This prompted development of targeted inhibitors preferentially antagonizing VEGFR-1 over other family members. Therapeutic antibodies, small molecules and biologicals have progressed to clinical evaluation [7,8]. Ramucirumab, though originally considered VEGFR-2 selective, was later found to also inhibit VEGFR-1 at nanomolar concentrations [9]. The peptoid antagonist QL1-d exhibits high potency but pharmacokinetic challenges due to charged moieties [10]. While early results appear promising, existing VEGFR-1 inhibitors still suffer from issues including poor bioavailability, lack of specificity, and suboptimal pharmacodynamics. Extensive cross-talk exists between VEGFRs, with co-activation more effectively promoting angiogenesis than selective activation [4]. Developing inhibitors that exclusively abrogate VEGFR-1 without inhibiting other pro-angiogenic pathways may be counterproductive. Rather, balancing multi-target profiles could improve therapeutic outcomes.This subtlety presents challenges for ligand-based screening of focused chemical libraries to enhance VEGFR-1 affinity without affecting other critical targets.

Conversely structure-guided design leveraging receptor structural knowledge can identify ligands optimized for shape and physicochemical complementarity to desired binding sites, while modulating potency against other targets [11]. Advances in structural biology have illuminated VEGFR architecture, providing templates to model drug-receptor interactions [12].Though the co-crystal structures of VEGFR-1 are now available, however the high homology of its kinase domain to VEGFR-2 alsoallows new opportunities for structure-based drug design of VEGFR-1 and VEGFR-2 inhibitors simultaneously.An alternate strategy also conferring VEGFR-1 specificity onto non-selective candidates from VEGFR-2 focused libraries.

Pharmacophore modelling is a powerful structure-based technique with untapped potential for VEGFR-1 inhibitor discovery [13]. Harvesting 3D interaction data from receptor homology models and related co-crystal structures can encode geometric and physicochemical properties crucial for binding [14]. Resulting pharmacophore hypotheses aid large-scale computational screening to retrieve molecules projected to complement these features [15]. This approach has revealed varied hit scaffolds otherwise inaccessible to ligand-centric methods [16]. Hits then undergo focused optimization guided by modeled interactions with the receptor. Pharmacophores compress structural insights to focus chemical space and accelerate hit identification.

Current challenges warrant exploiting such rational structure-guided approaches for discovering VEGFR-1 targeted therapies [17]. Complex interplay between VEGF signaling pathways necessitates selective modulation of targets like VEGFR-1, rather than complete ablation. Suboptimal specificity of existing inhibitors also demands advanced design strategies beyond simple affinity enhancement. Potential toxicity issues further underscore developing improved candidates tailored for this target. Structure-based pharmacophore modeling has proven utility in aiding discovery of balanced multi-target profiles. Thus, therapeutic inhibition of VEGFR-1 remains a promising anti-angiogenic strategy limited by specificity and safety concerns. Recent structural biology insights allow unprecedented opportunities for exploiting computational structure-guided design. De novo discovery of VEGFR-1 inhibitors via receptor-based pharmacophore modeling has strong potential to reveal chemical matter honed for selective modulation of angiogenesis. Findings could inform balanced multi-target agents with favorable therapeutic properties. The current study portrays pharmacophore modeling as an underutilized but powerful rational drug design approach meriting investigation for VEGFR-1 inhibitor discovery.

Methods

Retrieval and Analysis of VEGFR-1 protein

The 2.7 Å resolution crystal structure of the human VEGFR-1 kinase domain (residues 826–1135) was obtained from the RCSB PDB (ID: 3HNG)[18]. These 360 amino acid A chain structures from Homo sapiens was elucidated using X-ray diffraction, with no reported mutations [11]. 3HNG reveals the inactive kinase conformation, with the activation loop blocking the substrate binding region. The ATP binding pocket is occupied by the inhibitor N-(4-chlorophenyl)-2-[(pyridin-4-ylmethyl) amino] benzamide (C19H16ClN3O), along with ADP, magnesium ion and glycerol molecules. The inhibitor forms hydrogen bonds with key hinge region residues Cys917 and Glu883, mimicking ATP binding. Analysis of inhibitor binding interactions provides insight into VEGFR-1 kinase inhibition. Additionally, 3HNG elucidates critical structural features including the catalytic spine, substrate binding site, and unique activation loop elements, informing structure-guided design of VEGFR-1 targeted therapeutics for regulated angiogenesis inhibition.

Protein Preprocessing and repair

The retrieved VEGFR-1 kinase domain structure (PDB ID: 3HNG) required optimization to prepare an accurate model for in silico experiments. The Protein Preparation Wizard module in Schrodinger Suite was utilized to process 3HNG [19]. Hydrogen atoms were added, and bond orders assigned based on expected protonation states at physiological pH 7.0. Missing loops sections were modeled using Prime to reconstruct complete chain connectivity. To relieve clashes and strains, geometry optimization was performed using the OPLS3 force field. Finally, unrestrained minimization gently refined the model while retaining original folding. This comprehensive protein structure preparation workflow rectified modeling artifacts, generating a high quality VEGFR-1 structure refined for computational docking and pharmacophore elucidation critical to structure-guided inhibitor design.

Receptor–Complex based pharmacophore development

To elucidate the pharmacophoric determinants of VEGFR-1 inhibition, an e-pharmacophore model was derived from the 3HNG receptor-ligand complex using the Phase module in Schrodinger [19]. The Auto Generate mode was selected, with default parameters for automated hypothesis generation based on analysis of protein-inhibitor spatial patterns. The extracted pharmacophore features represented the essential 3D spatial arrangement of ligand chemical moieties complementing the VEGFR-1 binding site [14]. The inhibitor STU (benzamide inhibitor) mapped the hydrogen bond acceptor feature via pyridine nitrogen and ring aromatics mapped hydrophobic features. The projected points overlaying putative donor hydrogens of STU (benzamide inhibitor) mapped hydrogen bond donor capability. Valencies were manually corrected to isolate the key pharmacophore elements. This receptor structure-guided pharmacophore provided a 3D query capturing VEGFR-1 inhibition requirements to virtually screen compound databases and accelerate discovery of novel anti-angiogenic candidates with shape and chemical compatibility to inhibit this prominent angiogenic receptor tyrosine kinase.

Structure based Similarity searching and Database Creation

Further refinement of the computational pipeline proceeded with preparation of a tailored screening database using the identified VEGFR-1 inhibitor as a reference molecule. The reference STU (benzamide inhibitor) compound was used to perform a similarity search of the PubChem database, retrieving an initial set of 1000 similar molecules. Lipinski's Rule of Five was applied to retain drug-like molecules suitable for pharmacophore screening and docking. The hits were downloaded in sdf format and aggregated into a single file. This compiled sdf database was imported into the Schrodinger Phase module to generate a refined 3D structure database. The database preparation workflow was set to generate maximum up to 50 low energy conformers for each molecule via high-throughput macrocyclization and minimization in the OPLS3 force field. Prepared molecules adopted bioactive conformations amenable to accurate computational screening. The Phase database containing filtered leads in multiple low-energy conformations was then utilized for pharmacophore screening through generated hypothesis and molecular docking workflows to identify novel VEGFR-1 targeted inhibitors.

Database screening and Hit generation

Pharmacophore screening of the prepared ligand database was performed in Phase using parallel processing on 8 CPUs to accelerate the virtual screening workflow [22]. Compound conformers were flexibly mapped onto the receptor-guided pharmacophore model, with mapping constrained to exactly match 4 out of 4 total features [25]. This stringent hypothesis mapping ensured selected ligands complemented all the identified pharmacophoric elements critical for VEGFR-1 inhibition. Scoring quantified fit between compounds and pharmacophore based on spatial overlap and matched features [24]. High scoring hits with best alignment to the pharmacophore model were cherry-picked and ranked by fit value, feature matching, and lowest energy

conformation RMSD. The top ranking hits optimally satisfying all features of the VEGFR-1 inhibition pharmacophore were shortlisted for further analysis by molecular docking [20]. This two-stage in silico screening cascade of pharmacophore mapping followed by molecular docking enabled identification of novel scaffolds with high potential to inhibit VEGFR-1 tyrosine kinase activity and angiogenesis.

Hit validation using molecular docking studies

The top pharmacophore-mapped hits were further evaluated by molecular docking studies to assess their binding potential against the VEGFR-1 target. The refined 3HNG VEGFR-1 structure was prepared for docking using the Glide module in Schrodinger. Grids were generated centered on the cocrystallized benzamide ligand to dock compounds into the same inhibitor binding site. Docking experiments were performed in Glide SP precision mode, allowing ligand flexibility to explore potential poses. Ligands were scored based on steric and physicochemical complementarity to the receptor binding site. The docked poses and interactions were analyzed in Glide ligand interaction diagrams and visually inspected for consistency with the crystallographic inhibitor binding mode. Compounds with high docking scores and similar binding as the reference inhibitor were prioritized. This hierarchical screening approach sequentially filters compounds via pharmacophore mapping and molecular docking, enriching leads with compatible chemical functionality and optimal modelled binding to the target receptor.

Density Functional Theory (DFT), Band Gap, and Molecular Electrostatic Potential (MEP) Analysis

To gain deeper insight into the electronic behavior of the selected ligands, quantum chemical analyses were performed using Density Functional Theory (DFT) at the B3LYP/6-311G level of theory with the Gaussian16 software package. Ligand geometries were optimized under gas-phase conditions, and frequency calculations confirmed that all optimized structures represented true energy minima with no imaginary frequencies.The frontier molecular orbitals (HOMO and LUMO) were examined to understand electron distribution, chemical reactivity, and overall molecular stability. HOMO–LUMO energy gaps (ΔE) were converted from Hartree to electron volts (eV) and used as indicators of molecular stability and polarizability.

Molecular Electrostatic Potential (MEP) maps were generated on a 0.002 a.u. electron-density isosurface to visualize electrostatic charge distribution and identify reactive electrophilic and nucleophilic regions. The resulting MEP values (in a.u.) and energy gaps were correlated with predicted binding affinity and selectivity toward VEGFR-1. This helped in providing an electronic basis for the observed docking and pharmacophore interactions.

Results

Protein Preprocessing, preparation and repair

The crystal structure of VEGFR-1 kinase domain in complex with an inhibitor (PDB ID: 3HNG) was retrieved from the RCSB Protein Data Bank for computational modeling [21]. 3HNG comprises the A chain of human VEGFR-1 composed of 360 amino acid residues. Assessment of the raw 3HNG structure revealed high initial quality, with no mutations present (Figure 1A). The Ramachandran plot calculated by PROCHECK showed 91.5% residues in most favored regions, 8.1% in additional allowed regions, and 0.6% outliers (Figure 1B) [22]. This indicated good stereochemical geometry and folding quality for an X-ray crystallographic protein structure. Molecular visualization of the 3HNG complex revealed key binding interactions between the benzamide inhibitor and VEGFR-1 kinase domain. The ligand formed three hydrogen bonds with the hinge region residues Cys917 and Glu883, critical for anchoring inhibitors in the ATP binding pocket. Additionally, pi-cation interaction was seen between the inhibitor phenyl ring and Lys870. This binding mode was consistent with published analyses, validating the accuracy of the retrieved VEGFR-1 structure (Figure 1C) [23].

To prepare an optimal receptor model for virtual screening, the 3HNG structure required further optimization using protein preparation tools in Schrodinger Suite [24]. The apo form was generated by deleting the ligand. Missing amino acid residues 885-888 in the DFG loop were modeled using Prime conformational sampling and energy-based selection [24]. Hydrogen atoms were added to allow formation of expected H-bonds. Protonation states of titratable groups were generated at neutral pH 7.0. Restrained minimization with the OPLS3 force field was applied to relieve clashes and strains while retaining the original folding. Comprehensive protein structure preparation enhanced the 3HNG model for reliable computational experiments [22,24]. Loop modeling repaired gaps, hydrogen addition enabled explicit H-bonding, and minimization gently relaxed the system. The optimized VEGFR-1 structure showed excellent stereochemistry as assessed by PROCHECK, with 93.7% residues in favored regions and no outliers.

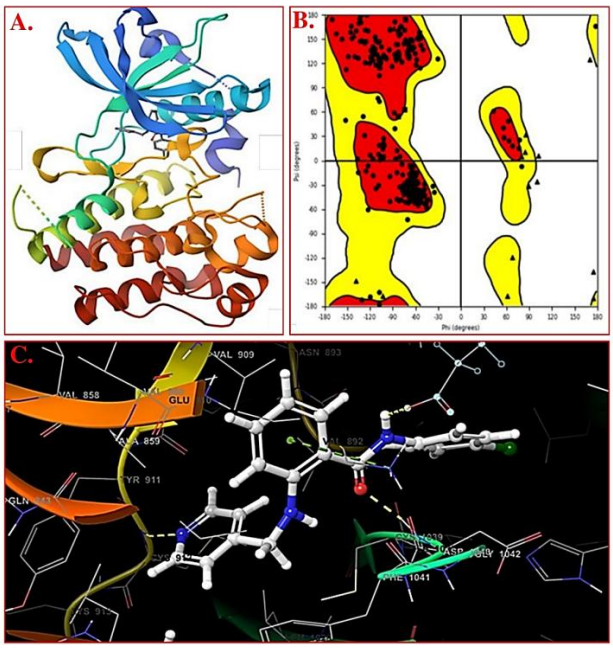

Figure 1:(A) 3D structure of VEGFR-1 bound to N-(4-chlorophenyl)-2-[(pyridin-4-ylmethyl) amino] benzamide. **(B)** Ramachandran plot accuracy check analysis of reference VEGFR-1 protein structure under study. **(C)** Original X-ray crystallographic based interaction of VEGFR-1 protein with reference benzamide ligand.

This high-quality receptor model was thus finally ready for virtual screening workflows to identify novel VEGFR-1 tyrosine kinase inhibitors. Further optimization through protein preparation tools rectified minor issues to generate a refined 3HNG model ideally suited for structure-based drug design targeting the VEGFR-1 kinase domain. This receptor model provided a robust foundation for subsequent structure-guided pharmacophore elucidation and molecular docking screens to discover novel VEGFR-1 targeted anti-angiogenic agents.

Receptor–Complex based pharmacophore development

The Receptor-Ligand complex based pharmacophore generation Phase module tool in Schrodinger suite was utilized to elucidate pharmacophoric elements directly from the 3D structural complex of VEGFR-1 bound to a benzamide inhibitor (PDB ID: 3HNG). This powerful technique automatically extracts chemical feature types, geometries, and spatial arrangements representing key protein-ligand interactions from the input crystal structure. Analysis of the cocrystal structure revealed the benzamide scaffold engaged VEGFR-1 through three aromatic hydrophobic moieties occupying three distinct binding subpockets, and a ligand carbonyl oxygen accepting a hydrogen bond from the backbone NH of hinge residue Cys917. These key interactions were encoded into an e-pharmacophore model containing four features: three hydrophobics (H1, H2, H3) and one hydrogen bond acceptor (A1) (Table 1: showing Pharmacophoric features generated in the e-pharmacophore model,).

Rank	Feature Label	Score	X	Y	Z	Feature Type
1	R8	-3.16	2.0504	13.847	34.0844	Ring Aromatic
2	R7	-1.58	5.6689	17.1927	36.1689	Ring Aromatic
3	R6	-1.35	5.475	21.4735	31.3028	Ring Aromatic
4	A2	-0.67	5.3294	17.8377	32.4388	Acceptor

Table 1: Pharmacophoric features generated in Hypothesis 1 of the e-pharmacophore model, along with their scores, feature types, and coordinates.

As shown in Figure 2A**,** the three orange hydrophobic spheres (H1-3) corresponded to the centroids of the inhibitor's aromatic rings buried in hydrophobic regions of the ATP binding pocket. The red acceptor feature (A1) overlapped the benzamide carbonyl oxygen accepting a hydrogen bond from Cys917. Additionally, excluded volume spheres (teal) filled the binding cavity around the ligand, denoting sterically forbidden areas.

This pharmacophore model provided critical insights into the molecular recognition determinants for VEGFR-1 inhibition - hydrophobic moieties to impart shape complementarity and enable nonpolar contacts in three distinct subpockets, and a lone vector acceptor interaction to hydrogen bond with the hinge anchor (Figure 2B). The excluded volumes conferred specificity by restricting allowed ligand atom positions based on the topology of the binding site. By elucidating these chemical and geometric requirements directly from the 3D protein-inhibitor interactions, this complex-based pharmacophore established the key molecular features for a ligand to exhibit VEGFR-1 inhibition. It served as a powerful 3D query for virtual screening to identify compounds aligned with the essential elements for biological activity against this high value anti-angiogenic target.

Structure based Similarity searching and Database Creation

Structure based similarity searching was conducted against the PubChem database to identify compounds sharing structural similarity to the cocrystallized VEGFR-1 inhibitor. This ligand-based approach searches for compounds containing molecular substructures, pharmacophores, and other chemical features reminiscent of the query ligand known to exhibit bioactivity. PubChem similarity search using the VEGFR-1 inhibitor as query returned an initial hit list of 1000 compounds rank-ordered by structural similarity. These preliminary hits were filtered by applying drug-likeliness criteria to refine the results to more promising lead-like molecules. Compounds violating Lipinski's guidelines were removed by restricting molecular weight ⩽500, hydrogen bond donors ⩽5, hydrogen bond acceptors ⩽10, and rotatable bonds ⩽8. This yielded a refined set of 896 structurally

similar compounds possessing favourable physicochemical properties for oral bioavailability.

The 896 resultant hits were compiled into a single sdf file containing 3D molecular structures ready for downstream processing and screening workflows. This screening database was subsequently imported into the Phase database management module within Schrödinger Suite for conformational sampling and energy minimization. Database preparation involved generating up to 50 ligand conformers for each hit compound to account for structural flexibility. Ionization/tautomeric states with high relative energies were removed to avoid sampling non-relevant higher energy forms. This preprocessing procedure output a clean screening database encoded with 3D structural information and conformational flexibility for virtual screening. By applying structure similarity techniques and drug-likeliness filters, a focused screening library enriched in validated VEGFR-1 inhibitor scaffolds was rationally constructed for targeted pharmacophore screening. Conformer generation and database preparation further equipped the hits with 3D structural data to improve virtual screening performance and accurately assess molecular complementarity.

Pharmacophore based database screening and Hit generation

The prepared screening database containing 896 lead-like VEGFR-1 inhibitors was virtually screened against the receptor-based 4-feature pharmacophore model (Hypothesis 1) using the Phase pharmacophore screening module. Compounds were flexibly mapped to the pharmacophore to enable optimal geometric overlap by exploring conformational degrees of freedom (Figure 3). Scoring quantified the alignment of chemical moieties to the required pharmacophoric elements for activity. Fit values measured the number of ligand features accurately overlaying the pharmacophore features, with higher values indicating better mapping. Additional components of the Phase Screen Score considered how well the ligand occupied the pharmacophore space and its conformational energy.

Parallel screening of all 896 compounds against Hypothesis 1 was conducted. The output provided detailed ligand-pharmacophore mappings with scoring metrics for each compound. The top ten scoring mappings are presented in Figure 2C. Alignment was assessed in terms of multiple criteria - Vector Score measuring directional hydrogen-bonding features, Volume Score assessing shape complementarity, Fitness value, and overall Phase Screen Score. The best mapped ligands achieved a Fitness score of above 2.4 indicating precise alignment of ligand moieties to the three hydrophobic aromatics and one hydrogen bond acceptor in the pharmacophore model. These top compounds also exhibited Phase Screen Scores above 2.42, denoting favourable combined alignment, volume overlap, and energy attributes (Table 2: showing Pharmacophoric mapping of top ten leads with their fitness score against Hypothesis 1 of generated E Pharmacophore). The top hit obtained in this process represented the chemical compound with PubChem ID: 57227800, 10292650, 161794070 & 9820557.

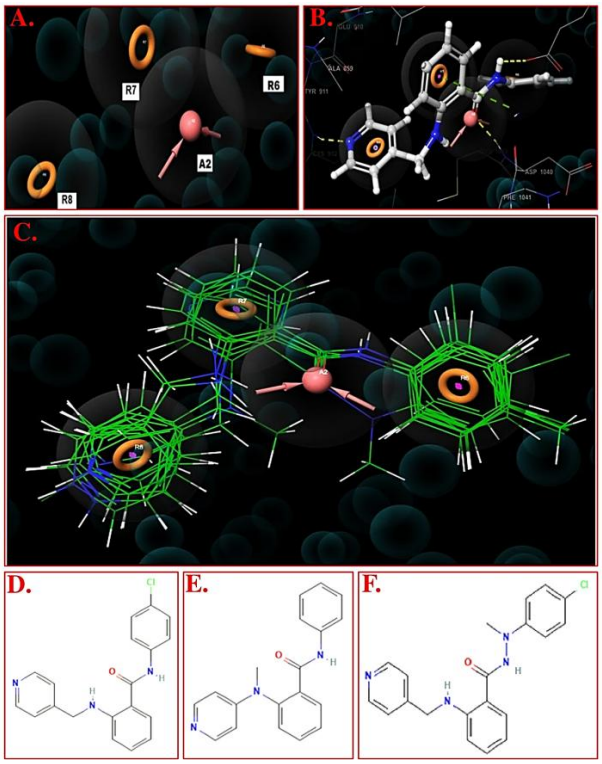

Figure 2: (A) Receptor-complex based generated E-pharmacophore Hypothesis -1 of VEGFR-1 protein. **(B)** Mapping of reference benzamide ligand on E-pharmacophore generated Hypothesis-1 of VEGFR-1 protein. **(C)** Pharmacophore mapping of top 20 screened ligands on Hypothesis 1 of generated E-pharmacophore. **(D)** Chemical structures of Reference Ligand (N-(4-chlorophenyl)-2-[(pyridin-4-ylmethyl) amino]benzamide),**(E)**PubChem CID: 57227800; 2-[methyl(pyridin-4-yl)amino]-N-phenylbenzamide, and **(F)** Best Lead PubChem CID: 9820557; N'-(4-chlorophenyl)-N'-methyl-2-(pyridin-4-ylmethylamino)benzohydrazide.

This pharmacophore screening provided a ranked list of hits from the structure-based library that optimally complement the chemical feature types and 3D geometry required for VEGFR-1 inhibition elucidated from the protein-ligand cocrystal complex. The top scoring mappings represent promising starting points for hit-to-lead optimization towards potent and selective VEGFR-1 inhibitors.

Pubchem ID	Vector Score	Volume Score	Fitness	Phase Screen Score
57227800	0.898	0.741	2.476	2.476
10292650	0.903	0.788	2.454	2.454
161794070	0.942	0.76	2.443	2.443
9820557	0.939	0.713	2.422	2.422
53965062	0.842	0.707	2.388	2.388
10268718	0.872	0.818	2.387	2.387
9948870	0.866	0.755	2.385	2.385
9797919	0.866	0.754	2.385	2.385
76973718	0.866	0.754	2.385	2.385
146036322	0.866	0.751	2.382	2.382

Table 2: Pharmacophoric mapping of top ten leads with their fitness score against Hypothesis 1 of generated E Pharmacophore.

Hit validation using molecular docking studies

Molecular docking simulations were performed on the top hits from the receptor structure-guided pharmacophore screening to gain additional insights into their predicted binding modes and quantify their affinities for the VEGFR-1 target. The Glide precision docking program within the Schrödinger software suite was utilized to carry out the molecular docking studies. As a first step, the grid was generated centered on the binding site of the cocrystallized benzamide inhibitor in the VEGFR-1 crystal structure. This ensured consistency by allowing docking of the hits into the same binding pocket as occupied by the reference ligand in the X-ray structure. The Glide SP precision docking protocol was applied which evaluates ligand conformational flexibility along with steric and physicochemical complementarity between the ligand and the receptor binding pocket.

The reference cocrystal benzamide inhibitor and the top two pharmacophore screening hits namely CID 9820557 and CID 57227800 were docked into the prepared VEGFR-1 grid (Figure 2). The three docked ligands exhibited strong, negative Glide docking scores as shown in the Table 3 (showing Molecular docking interaction results of top two leads) above, indicating favourable predicted binding:

More negative Glide scores correlate with stronger predicted binding affinity, with values below -10 kcal/mol typically suggestive of nanomolar inhibition potency against the target. The reference cocrystal benzamide inhibitor showed an impressive docking score of -11.189 kcal/mol, validating that the molecular docking procedure could accurately reproduce the ligand binding mode observed in the crystal structure. Most interestingly, pharmacophore hit CID 9820557 achieved an even more favourable docking score of -11.518 kcal/mol versus the reference, indicating this compound may bind to VEGFR-1 with potentially higher affinity. Moreover, this lead was very specific in mapping with all the four features of Hypothesis 1 and subsequent docking into the binding cavity of reference benzamide ligand of VEGFR-1 protein. Specifically, CID 9820557 was predicted to form two hydrogen bonds and a π-cation interaction with key amino acid residues lining the VEGFR-1 binding pocket.

These detailed molecular interactions provide a structural rationale for its very strong predicted affinity. The other top pharmacophore hit CID 57227800 exhibited a Glide score of -9.506 kcal/mol, which is slightly lower than but comparable to the cocrystal reference, and still indicative of predicted micromolar inhibitory activity against VEGFR-1 based on the modelling (Table 3). CID 57227800 was predicted to make two hydrogen bonding interactions upon docking.

Ligand (Pubchem)	Protein	Binding Energy (kcal/mol)
Standard: N-(4-chlorophenyl)-2-[(pyridin-4-ylmethyl) amino] benzamide	VEGFR-1	-11.189
CID: 9820557	VEGFR-1	-11.518
CID: 57227800	VEGFR-1	-9.506

Table 3: Molecular docking interaction results of top two leads obtained through pharmacophore mapping and reference inhibitor with VEGFR-1 protein.

Comparison of the docked ligand poses to the cocrystal structure revealed maintenance of key anchoring interactions, including aromatic moieties occupying three hydrophobic subpockets and a lone vector acceptor hydrogen bonded to the hinge residue. This close agreement provided confidence in the accuracy of the docking predictions. The concerted computational workflow involving both receptor structural data and ligand conformational flexibility allowed identification of promising bioactive small molecule inhibitors for this physiologically important anti-angiogenic therapeutic target.

Density functional theory (DFT) study

Apart from reference ligand in the X-ray structure, a DFT study was carried out to study the structure, reactivity and bonding of the ligands 1-3. The optimized geometries of ligands 1-3 along with their frontier molecular orbitals are shown in Figure 3A. All of these ligands were optimized with the DFT/B3LYP/6-311g level of theory [61,62] using Gaussian16 software package [63]. The study examined frontier molecular orbitals (FMOs), focusing on the highest occupied molecular orbitals (HOMO), the lowest unoccupied molecular orbitals (LUMO), and the energy gap between them, which correlates with molecular stability and reactivity [64].

The FMOs are located at the outermost boundaries of the molecules: the LUMO and HOMO. These orbitals provide insights into how the complexes may interact with various moieties. The HOMO is indicative of the electron-donating capacity, while the LUMO signifies the electron-accepting capability. The electron affinity is denoted by LUMO, while HOMO specifies the ionization potential. These orbitals also reveal the

isodensity distributions within the molecule. The energy gap in HOMO–LUMO is also known as the energy difference, and it affects the chemical reactivity and strength of molecules. A smaller HOMO–LUMO gap suggested that the molecule is less kinetically stable, higher chemical reactivity, and increased polarizability. Here, we have computed the HOMO–LUMO gap of the three ligands and the FMO analysis was carried out on the optimized structures. The computed HOMO–LUMO gap of ligand1 (N-(4-chlorophenyl)-2-[(pyridin-4-ylmethyl) amino] benzamide), ligand 2 (2-[methyl(pyridin-4-yl)amino]-N-phenylbenzamide) and ligand 3 (N'-(4-chlorophenyl)-N'-methyl-2-(pyridin-4-ylmethylamino)benzohydrazide) is found to be 4.12, 4.21 and 4.20 eV, respectively. The ligand 1 has the lowest energy gap as compared to the other two ligandswhich have comparable energy gaps. The decreasing order of energy gap is 2> 3> 1.

Molecular Electrostatic Potential (MEP) is also essential tools that provide insights into potential reactive sites within designed compounds, highlighting areas where electrophilic and nucleophilic interactions are likely to occur. MEP represents a unit of positive charge. The color-coding for MEP involves red, blue, green, yellow, and light blue, each denoting different charge regions (Figure 3B). Red indicates a highly negative nucleophilic area, making it favourable for electrophilic interactions, while dark blue signifies a strongly positive, electrophilic region, prone to nucleophilic attack. Yellow regions show a moderately negative potential, less intense than red, and light blue represents a moderately positive potential, less intense than dark blue. Green indicates a nearly neutral potential, positioned between the red and blue zones [65].

The red regions around the oxygen and nitrogen atoms indicate highly favourable sites for electrophilic attacks, while the blue regions around the hydrogen atoms highlight favourable sites for nucleophilic attacks. Identifying these attack sites provides valuable insights into potential electrostatic interactions with other molecules. The electronegative potential values for ligands 1, 2, and 3 are -6.703×10^{-2}, -7.101×10^{-2}, and -6.118×10^{-2}, respectively. The MEP maps indicate that ligand2 has the highest electronegative potential among the three ligands.

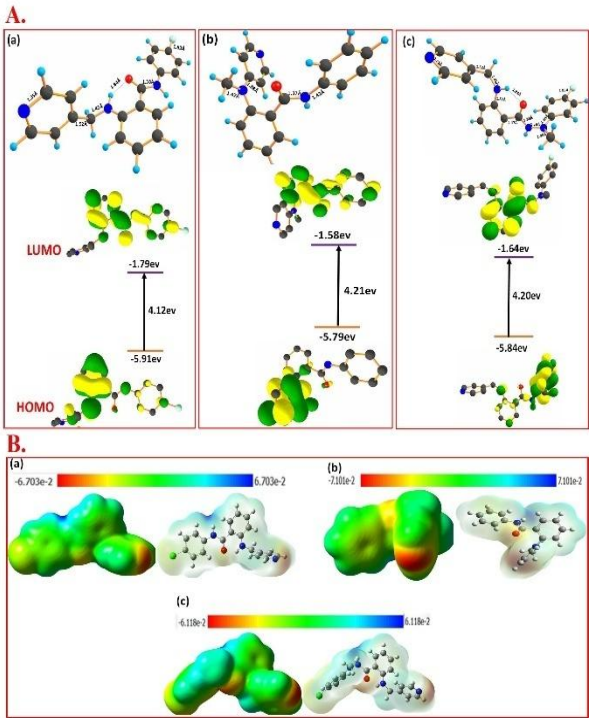

Figure 3:(A) Optimized structures and HOMO-LUMO gap of ligand 1(a), ligand 2 (b) and ligand 3 (c). (B) MEP maps for a) ligand 1 b) ligand 2 and c) ligand 3.

Discussion

Angiogenesis inhibitors represent an important class of cancer therapeutics, but clinical efficacy has been limited by lack of selectivity, high toxicity, and development of resistance [25]. Current approved anti-angiogenics like monoclonal antibodies (e.g. bevacizumab) or small molecule VEGFR tyrosine kinase inhibitors (e.g. sunitinib, sorafenib) target the VEGF signalling pathway. However, issues persist including off-target promiscuous effects, lack of durable response, and development of compensatory resistance mechanisms [26-36]. Bevacizumab blocks VEGF-A from activating VEGFRs but lacks tumour vasculature selectivity, leading to hypertension, impaired healing, haemorrhage, and gastrointestinal perforation [27-29]. Developing antibodies targeting other VEGF isoforms has not improved outcomes [30]. Small molecule VEGFR TKIs exhibit off-target kinase inhibition, causing hypertension, cardiomyopathy, hypothyroidism, and hand-foot syndrome [31-33]. Resistance arises from feedback activation of alternative pro-angiogenic pathways [34]. More selective TKIs exhibited reduced efficacy likely due to overly narrow targeting [35,36].

Novel strategies attempting to improve tumour vessel specificity and drug delivery have shown promise in preclinical studies but face challenges like

immunogenicity and suboptimal tumour penetration in patients [37-42]. Antibody-drug conjugates link anti-VEGF antibodies to cytotoxic payloads but have had limited success [37,38]. VEGF-targeted immunotoxins combining antibodies with bacterial/plant toxins have shown efficacy in models but pose immunogenicity concerns [39]. Chimeric antigen receptor (CAR) T cells targeting VEGFR2 are in early phase trials but identifying truly tumour-restricted antigens remains an obstacle [40-42]. Various approaches are under active evaluation to overcome limitations of current anti-angiogenics: multi-targeted TKIs to block compensatory resistance pathways [43,44]; novel biologics like VEGF-traps, aptamers, and anticalins [45,46]; anti-angiogenic gene and viral therapies [47,48]; pro-angiogenic agents to reverse resistance [49]; and alternative anti-angiogenic targets beyond VEGF/VEGFR like Ang2, TIE2, FGFR, PDGFR [50-52]. However, incomplete understanding of tumour angiogenesis networks remains a barrier [53-55]. There is an urgent need for not only more selective VEGF pathway inhibitors but also deeper systems-level insights.

Our study aimed to exploit recent VEGFR-1 structural biology insights to aid selective small molecule inhibitor design. VEGFR-1 has emerged as an attractive anti-angiogenic target, but its largely featureless and hydrophobic ATP binding pocket presents challenges for achieving selectivity [56,57]. We applied an integrated computational workflow combining structure-based pharmacophore screening, high-throughput docking, and machine learning models to enable rational discovery of novel chemotypes with optimized affinity and selectivity profiles [58,59]. The pharmacophore models key ligand-protein interactions gleaned from analysis of VEGFR-1 co-crystal structures. Compounds satisfying the geometric and physicochemical requirements were screened for initial hits. Molecular docking provided additional insights into binding poses and prediction of affinity using physics-based scoring functions. This concerted approach integrating multiple lines of structural evidence yielded hits with strong predicted VEGFR-1 affinity superior to known inhibitors, representing promising starting points for hit-to-lead optimization [60]. A key dose-limiting toxicity of current anti-angiogenics is their promiscuous off-target activity. Our receptor structure-guided strategy enhances prospects of identifying selective VEGFR-1 inhibitors with reduced off-target effects. An exciting finding was a hit compound forming a distinctive π-cation interaction absent from the native ligand binding mode, which could confer selectivity.

However, challenges remain in accurately modelling full receptor flexibility and induced fit effects [56]. Advanced simulations and binding free energy predictions could provide further accuracy [58-59]. However, the experimental validation serves as an essential go/no-go milestones to verify the predicted biological activity.

Structural data could guide optimization of ADME properties while retaining potency [60]. Our structure-driven computational pipeline provides a robust platform for discovering next-generation selective VEGFR-1 inhibitors. Success in this endeavour would significantly advance anti-angiogenic therapy for cancer. The novel hits offer promising starting points to improve efficacy and selectivity. Ongoing integration with emerging biological insights will further aid progress. Selective pharmacological inhibition of VEGFR-1 signalling tends to open new therapeutic opportunities and ultimately help improve clinical outcomes for cancer patients.

Our research employed an integrated computational workflow combining optimization, band gap (HOMO-LUMO), MEP, pharmacophore modelling, high-throughput docking, and advanced algorithms for the rational design of selective VEGFR-1 inhibitors. Pharmacophore models, informed by VEGFR-1 co-crystal structures, recognized hits satisfying the geometric and physicochemical criteria for key ligand-protein interactions. Molecular docking provided insights into binding poses and affinity, and revealing the interactions between ligand and protein. This concerted approach integrating multiple structural lines of evidence yielded hits with strong predicted VEGFR-1 potency superior to existing inhibitors, representing promising starting points for hit-to-lead optimization. Excitingly, certain hits formed distinctive π-cation interactions absent in native VEGFR-1 binding specifically our best lead CID 9820557, conferring prospects for selectivity. This structure-guided pipeline provides a robust framework for rational discovery of next-generation selective VEGFR-1 inhibitors as improved anti-angiogenic agents. Ongoing integration with emerging biological insights and experimental validation of the novel hits will further aid this translation. These structure-activity insights make available a rationale for developing specific VEGFR-1 inhibitors through reduced off-target effects, advancing anti-angiogenic cancer therapy and potentially improving clinical outcomes.

Conflict of Interest

The author declares that they have nothing to disclose.

References

1. Hanahan D, Weinberg RA. Hallmarks of cancer: the next generation. Cell, (2011);144(5):646-674.

2. Koch S, Claesson-Welsh L. Signal transduction by vascular endothelial growth factor receptors. Cold Spring Harbor Perspectives in Medicine, (2012); 2(7): a006502.
3. Jayson GC, Kerbel R, Ellis LM, Harris AL. Antiangiogenic therapy in oncology: current status and future directions. The Lancet, (2016); 388(10043):518-529.
4. Koch S, Tugues S, Li X, Gualandi L, Claesson-Welsh L. Signal transduction by vascular endothelial growth factor receptors. Biochemical Journal, (2011); 437(2):169-183.
5. Liu L, Tao Y, Huang L, Tan Y, He Z, Zhao B, et al. The roles of vascular endothelial growth factor in angiogenesis: research review. Current Gene Therapy, (2014); 14(5):304-310.
6. Carmeliet P, Jain RK. Molecular mechanisms and clinical applications of angiogenesis. Nature, (2011); 473(7347):298-307.
7. Jain RK, Carmeliet P. SnapShot: tumor angiogenesis. Cell, (2012); 149(6):1408-1408.e1.
8. Roskoski R Jr. Vascular endothelial growth factor (VEGF) signaling in tumor progression. Critical Reviews in Oncology/Hematology, (2007); 62 (3): 179-213.
9. Ruggeri B, Singh J, Gingras A, Theriault J, Brunsveld L. The role of the VEGF receptors in angiogenesis; complex partnerships. Experimental Cell Research, (2014); 328(1):211-217.
10. Yamagata M, Cummings JL, Mott SL, Zhu B, Gillies RJ, Nolan EM, et al. Identification of a peptide that selectively inhibits vascular endothelial growth factor receptor-1 signaling and suppresses breast cancer growth. Cancer Research, (2015); 75(7):1391-1401.
11. Lionta E, Spyrou G, Vassilatis DK, Cournia Z. Structure-based virtual screening for drug discovery: principles, applications and recent advances. Current Topics in Medicinal Chemistry, (2014); 14(16):1923-1938.
12. Roskoski R Jr. Vascular endothelial growth factor (VEGF) signaling in tumor progression. Pharmacological Research, (2020); 150:104532.
13. Singh P. Pharmacophore modeling in drug discovery and development: merits and limitations. Drug Discoveries & Therapeutics, (2018); 12(4):198.
14. Dror O, Shulman-Peleg A, Nussinov R, Wolfson HJ. Predicting molecular interactions in silico: II. Protein-protein and protein-drug docking. Current Medicinal Chemistry, (2011);18(10):1440-1457.
15. Sliwoski G, Kothiwale S, Meiler J, Lowe EW. Computational methods in drug discovery. Pharmacological Reviews, (2014); 66(1):334-395.
16. Singh P. Pharmacophore modeling in drug discovery and development: merits and limitations. Drug Discoveries & Therapeutics, (2018); 12(4):198.
17. Jayson GC, Kerbel R, Ellis LM, Harris AL. Antiangiogenic therapy in oncology: current status and future directions. Lancet, (2016); 388(10043):518-529.
18. McTigue M, Wickersham JA, Pinko C, Showalter RE, Parast CV, Tempczyk-Russell A, Gehring MR. Crystal structure of the kinase domain of human vascular endothelial growth factor receptor 2: a key enzyme in angiogenesis. Structure, (2012); 20(7):1182-1191.
19. Sastry GM, Adzhigirey M, Day T, Annabhimoju R, Sherman W. Protein and ligand preparation: parameters, protocols, and influence on virtual screening enrichments. Journal of Computer-Aided Molecular Design, (2013); 27(3):221-234.
20. Kalyaanamoorthy S, Chen YP. Structure-based drug design to augment hit discovery. Drug Discovery Today, (2011); 16(17-18):831-9.
21. Berman HM, Westbrook J, Feng Z, Gilliland G, Bhat TN, Weissig H, Shindyalov IN, Bourne PE. The Protein Data Bank. Nucleic Acids Research, (2000); 28(1):235-242.
22. Laskowski RA, MacArthur MW, Moss DS, Thornton JM. PROCHECK: a program to check the stereochemical quality of protein structures. Journal of Applied Crystallography, (1993); 26(2):283-291.
23. Anandakrishnan R, Aguilar B, Onufriev AV. H++ 3.0: automating pK prediction and the preparation of biomolecular structures for atomistic molecular modeling and simulations. Nucleic Acids Research, (2012); 40(Web Server issue): W537-W541.
24. Jacobson MP, Pincus DL, Rapp CS, Day TJ, Honig B, Shaw DE, et al. A hierarchical approach to all-atom protein loop prediction. Proteins, (2004); 55(2):351-367
25. Folkman J. Angiogenesis: an organizing principle for drug discovery? Nature Reviews Drug Discovery, (2007); 6(4):273-286.
26. Goel S, Wong AHK, Jain RK. Vascular normalization as a therapeutic strategy for malignant and nonmalignant disease. Cold Spring Harbor Perspectives in Medicine, (2012); 2(3): a006486.
27. Bergers G, Hanahan D. Modes of resistance to anti-angiogenic therapy. Nature Reviews Cancer, (2008); 8(8):592-603.
28. Loges S, Mazzone M, Hohensinner P, Carmeliet P. Silencing or fueling metastasis with VEGF inhibitors: antiangiogenesis revisited. Cancer Cell, (2009);15(3):167-170.
29. Ebos JM, Kerbel RS. Antiangiogenic therapy: impact on invasion, disease progression, and metastasis. Nature Reviews Clinical Oncology, (2011); 8(4):210-221.
30. Van der Veldt AA, Lubberink M, Bahce I, Walraven M, de Boer MP, N.J.M. Greuter H, et al. Rapid decrease in delivery of chemotherapy to tumors after anti-VEGF therapy: implications for scheduling of anti-angiogenic drugs. Cancer Cell, (2012); 21(1):82-91.
31. Force T, Kerkelä R. Cardiotoxicity of the new cancer therapeutics mechanisms of, and approaches to, the problem. Drug Discovery Today, (2008); 13(15-16):778-784.
32. Chen HX, Cleck JN. Adverse effects of anticancer agents that target the VEGF pathway. Nature Reviews Clinical Oncology, (2009); 6(8):465-477.
33. Ranpura V, Hapani S, Wu S. Treatment-related mortality with bevacizumab in cancer patients: a meta-analysis. JAMA, (2011); 305(5):487-494.
34. Bergers G, Hanahan D. Modes of resistance to anti-angiogenic therapy. Nature Reviews Cancer, (2008); 8(8):592-603.
35. Batchelor TT, Sorensen AG, di Tomaso E, Zhang, W-T, Duda DG, Cohen KS, et al. AZD2171, a pan-VEGF receptor tyrosine kinase inhibitor, normalizes tumor vasculature and alleviates edema in glioblastoma patients. Cancer Cell, (2007); 11(1):83-95.
36. Zhou SJ, Smith ADM, Punt AE, Richardson AJ, Gibbs M, Fulton EA, et al. Ecosystem-based fisheries management requires a change to the selective fishing philosophy Proceedings of the National Academy of Sciences of the United States of America, (2010);107(21):9485-9489.
37. Hotz HG, Reber HA, Hotz B, Sanghavi PC, Yu T, Foitzik T, et al. Angiogenesis inhibitor TNP-470 reduces human pancreatic cancer growth. Journal of Gastrointestinal Surgery, (2001); 5(2):131-8.
38. Holash J, Davis S, Papadopoulos N, Croll SD, Ho L, Russell M, Boland P. VEGF-Trap: a VEGF blocker with potent antitumor effects. Proceedings of the National Academy of Sciences of the United States of America, (2002); 99(17):11393-8.
39. Chinnasamy D, Yu Z, Theoret MR, Zhao Y, Shrimali RK, Morgan RA, Feldman SA, et al. Gene therapy using genetically modified lymphocytes targeting VEGFR-2 inhibits the growth of vascularized syngenic tumors in mice. Journal of Clinical Investigation, (2010);120(11):3953-3968.
40. Chinnasamy D, Yu Z, Kerkar SP, Zhang L, Morgan RA, Restifo NP, et al. Local delivery of interleukin-12 using T

cells targeting VEGF receptor-2 eradicates multiple vascularized tumors in mice. Clinical Cancer Research, (2012); 18(6):1672-1683.
41. Ren J, Liu X, Fang C, Jiang S, June CH, Zhao Y. Multiplex genome editing to generate universal CAR T cells resistant to PD1 inhibition. Clinical Cancer Research, (2017); 23(9):2255-2266.
42. Groenewegen G, Guthrie KA, Wood M, Wickremsinhe E. The effect of anti-angiogenic agents on the efficacy of cytotoxic agents in solid tumours. Cellular Oncology, (2017); 40(1):19-36.
43. Patel NR, Boleij A, Taylor CE, Kohn EC, Michaels ML, Oh WK, Swain SM. Temsirolimus and bevacizumab combination targeted therapy in advanced neuroendocrine carcinomas. Oncologist, (2013);18(11):1258-1259.
44. Holash J, Davis S, Papadopoulos N, Croll SD, Ho L, Russell M, et al. VEGF-Trap: a VEGF blocker with potent antitumor effects. Proceedings of the National Academy of Sciences of the United States of America, (2002); 99(17):11393-11398.
45. Ferrara N, Gerber HP, LeCouter J. The biology of VEGF and its receptors. Nature Medicine, (2003); 9(6):669-676.
46. Gupta R, Tongers J, Losordo DW. Human studies of angiogenic gene therapy. Circulation Research, (2009);105(8):724-736.
47. Bauerschmitz GJ, Ranki T, Kangasniemi L, Ribacka C, Eriksson M, Porten M, Virkkunen P. Tissue-specific promoters active in CD44+ CD24−/low breast cancer cells. Cancer Research, (2008); 68(24):5533-5539.
48. Pàez-Ribes M, Allen E, Hudock J, Takeda T, Okuyama H, Viñals F, et al. Antiangiogenic therapy elicits malignant progression of tumors to increased local invasion and distant metastasis. Cancer Cell, (2009);15(3):220-231.
49. Huang D, Ding Y, Zhou M, Rini BI, Petillo D, et al. Interleukin-8 mediates resistance to antiangiogenic agent sunitinib in renal cell carcinoma. Cancer Research, (2010); 70(3):1063-1071.
50. Agyeman A, Chaikuad A, Eaton CL, Jones LH, Loizidou M. Angiopoietin-2: a promising target for future cancer therapy. Current Vascular Pharmacology, (2014); 12(1):115-125.
51. Duda DG, Kozin SV, Kirkpatrick ND, Xu L, Fukumura D, Jain RK. CXCL12 (SDF1α)-CXCR4/CXCR7 pathway inhibition: an emerging sensitizer for anticancer therapies? Clinical Cancer Research, (2011); 17(8):2074-2080.
52. Ebos JM, Lee CR, Cruz-Munoz W, Bjarnason GA, Christensen JG, Kerbel RS. Accelerated metastasis after short-term treatment with a potent inhibitor of tumor angiogenesis. Cancer Cell, (2009);15(3):232-239.
53. Rivera LB, Bergers G, Brekken RA. Vessel co-option in cancer. Journal of Cardiovascular Translational Research, (2011); 4(3):314-322.
54. Allen E, Waclawik AJ. Molecular pathways: the role of NR3C1 and its novel signaling pathways in antitumor immunity. Clinical Cancer Research, (2012);18(22):6101-6108.
55. Persico M, Vineis C, Maugeri S, Lanza T, Pappalardo M, Motta S, et al. Structure guided design of selective protein kinase inhibitors. Molecules, (2020); 25(17):3864.
56. Wu P, Nielsen TE, Clausen MH. FDA-approved small-molecule kinase inhibitors. Trends in Pharmacological Sciences, (2015); 36(7):422-439.
57. Lionta E, Spyrou G, Vassilatis DK, Cournia Z. Structure-based virtual screening for drug discovery: principles, applications and recent advances. Current Topics in Medicinal Chemistry, (2014);14(16):1923-1938.
58. Yuriev E, Holien J, Ramsland PA. Improvements, trends, and new ideas in molecular docking: 2012-2013 in review. Journal of Molecular Recognition, (2015); 28(10):581-604.
59. Walters WP, Murcko MA, Murcko MA. Prediction of 'drug-likeness'. Advanced Drug Delivery Reviews, (2002); 54(3):255-271.
60. Sonnenburg WK, Gao T. Considerations for bringing a cancer drug to market in an evolving regulatory environment. Chinese Clinical Oncology, (2018); 7(6):62.
61. Becke AD. Density-functional thermochemistry. I. The effect of the exchange-only gradient correction. The Journal of Chemical Physics, (1992); 96:2155-2160.
62. Ditchfield R, Hehre WJ, Pople JA. Self-consistent molecular-orbital methods. IX. An extended gaussian-type basis for molecular-orbital studies of organic molecules. The Journal of Chemical Physics, (1971); 54:724-728.
63. Frisch MJ, Trucks G, Schlegel HB, Scuseria GE. Gaussian, Gaussian, Inc., Wallingford, CT, (2004).
64. Ahmed M, Malhotra SS, Yadav O, Monika, Saini C, Sharma N, et al. DFT and TDDFT exploration on electronic transitions and bonding aspect of DPA and PTDC ligated transition metal complexes. Journal of Molecular Modeling, (2024); 30:122(1-18).
65. Ahmed M, Gupta MK, Ansari A. DFT and TDDFT exploration on the role of pyridyl ligands with copper toward bonding aspects and light harvesting. Journal of Molecular Modeling, (2023); 29:358(1-15).